


Article

A New Calculation Method of Cutterhead Torque Considering Shield Rolling Angle

Xiang Shen ¹, Dajun Yuan ², Dalong Jin ² and Chengyong Cao ^{3,4,*} 

¹ College of Civil and Transportation Engineering, Shenzhen University, Shenzhen 518060, China; shenxiang@szu.edu.cn

² Key Laboratory of Urban Underground Engineering of Ministry of Education, Beijing Jiaotong University, Beijing 100044, China; djyuan@bjtu.edu.cn (D.Y.); dljin@bjtu.edu.cn (D.J.)

³ Key Laboratory for Resilient Infrastructures of Coastal Cities (MOE), Shenzhen University, Shenzhen 518060, China

⁴ Shenzhen Key Laboratory of Green, Efficient and Intelligent Construction of Underground Metro Station, Shenzhen 518060, China

* Correspondence: chengyongcao@163.com; Tel.: +86-18001066820

Abstract: The existing cutterhead torque calculation method usually simplifies the characteristics of the shield, which ignores the rolling angle. In this paper, the cross-river shield project of Wuhan Metro Line 8 is taken as the research focus. Firstly, the measured data of the cutterhead torque (CT), the rolling angle and rotation direction were analyzed. Then on this basis, the penetrability, tunneling thrust, and rolling angle were taken as the influential factors to analyze CT sensitivity. Finally, based on the theoretical calculation model, a modified solution of CT was obtained considering the rolling angle. The results show that the rolling angle can be reduced to zero by changing the direction of the cutterhead rotation; the rolling angle has a greater impact on CT than the other two factors as shown through the analysis of the range difference and Statistical Product and Service Solutions (SPSS) method. As the absolute value of the rolling angle increases, CT also increases, and the relationship between them is linear. To a certain extent, the rolling angle of the shield can reflect the difficulty of tunneling and the running status. By monitoring the rolling angle of the shield, the prediction of CT can be more in line with the actual construction conditions.

Keywords: shield tunnel; rolling angle; cutterhead torque (CT); correlation analysis; modified solution



Citation: Shen, X.; Yuan, D.; Jin, D.; Cao, C. A New Calculation Method of Cutterhead Torque Considering Shield Rolling Angle. *Appl. Sci.* **2022**, *12*, 396. <https://doi.org/10.3390/app12010396>

Academic Editor: Daniel Dias

Received: 30 September 2021

Accepted: 28 December 2021

Published: 31 December 2021

Publisher's Note: MDPI stays neutral with regard to jurisdictional claims in published maps and institutional affiliations.



Copyright: © 2021 by the authors. Licensee MDPI, Basel, Switzerland. This article is an open access article distributed under the terms and conditions of the Creative Commons Attribution (CC BY) license (<https://creativecommons.org/licenses/by/4.0/>).

1. Introduction

Due to the advantages of being unaffected by the climate, stable traffic capacity, strong resistance to war damage and to damage from shipping, underwater tunnels have increasingly become an important means of connection and a traffic lifeline between cities, regions, and even countries [1–3]. During long-distance tunneling using large-diameter shields, cutter wear and attitude control have a significant impact on the safety of tunneling [4,5]. Tunnel Boring Machine (TBM) tunneling is affected by complex factors, such as the soil properties, the water and soil pressure, the jack thrust, and the cutterhead torque (CT) [6,7]. Proving the dynamic mechanism of the interaction between machine and soil is a prerequisite for optimal control of shield construction mechanics [8].

CT is an important part of shield tunneling parameters [9,10]. It is related to whether the shield tunneling can be carried out with high efficiency. However, CT is affected by many factors such as the type of shield, the form of the cutterhead, the type of cutter, and the formation conditions. In recent years, as the diameter of shields continues to increase, CT is also increasing, and the gap between the maximum value of the cutterhead torque and the average value is also increasing in these projects. Therefore, it is very important to study the characteristics of CT and its influencing factors, and establish the two-way relationship

between the soil and the shield, which can lay the foundation for the establishment of the mathematical model of CT [11,12].

At present, the empirical formula widely used in shield design and construction areas is that proposed by Krause [13]. In view of the fact that the empirical formula could have too many considerations, it is mainly based on the statistical results of a large number of construction data, ignoring the influence of complex formation conditions and machine parameters on CT. Reilly [14] proposed an empirical formula to determine CT, but there still exist large uncertainties in this model. Therefore, in recent decades, many attempts have been made to establish a cutterhead torque prediction method based on physical models [15,16]. Taking account of cutterhead structure, cutting principle and the interaction between cutterhead and soil composition, and corresponding calculation method of cutterhead torque as presented by Shi et al. [17]. Wang et al. [18] proposed a new calculation model considering dynamic parameters, which was verified by laboratory tests, and established a shield load prediction model for cutterhead torque and thrust. Zhang et al. [19] established a shield load prediction model for cutterhead torque and thrust, taking into account the influence of the shield-soil interaction. Ates et al. [20] collected 262 TBMs' design parameters, and analyzed the relationship between TBM diameter and installed thrust capacity, nominal torque, and others. With the continuous development of shield tunnel technology, shield engineering will have to face a variety of geological conditions. González et al. [21] proposed a calculation model suitable for soils and soft rock, and Zhou and Zhai [22] extended the existing theory to mixed-face ground. Although methods based on physical models can predict the CT trend, there are still many key factors that have not been considered, such as cutterhead rotation, advance speed, total thrust, and torque. Moreover, the theoretical calculation methods mentioned above are only suitable for specific cutterhead design and geological conditions.

Due to the low accuracy of the theoretical calculation method of cutterhead torque, machine learning has been widely used in the prediction of tunnelling parameters [23,24]. First, a large number of tunneling parameters need to be analyzed initially. In recent years, Statistical Product and Service Solutions (SPSS) is often used in data analysis in civil engineering [25,26]. Three intelligent models were employed to predict advance speed, torque, thrust, and other operating parameters, including a predeveloped artificial neural network (ANN), hybrid particle swarm optimization (PSO)-ANN, and a hybrid imperialist competitive algorithm (ICA)-ANN [27–29]. Luo et al. [30] proposed an optimal control method for slurry pressure based on random forest (RF) and particle swarm optimization (PSO). Qin et al. [31] proposed an approach of precise cutterhead torque prediction for shield tunneling machines using a novel hybrid deep neural network. Shi et al. [32] proposed a novel VMD-EWT-LSTM-based multi-step prediction method for shield machine cutterhead torque. Although these algorithms can achieve better prediction accuracy, the methods require more data as the basic database for the prediction model. From the existing research results, more analysis is based on the data of the entire project.

Based on the above literature review, the empirical calculation model of cutterhead torque is only a reference, and there is often a large error with the actual measured value. The existing theoretical calculation model of cutterhead torque is generally only applicable to a single formation. Machine learning prediction models require large amounts of data as a basis. To resolve these problems, this paper aims to establish a calculation method of cutterhead torque considering the rolling angle. Based on the Wuhan Metro Line 8 project, a large amount of engineering data has been collected. Through the analysis of factors and SPSS, the correlation between tunneling speed, rotation speed, tunneling thrust, rolling angle, and cutterhead torque is analyzed. Based on a physical mechanics model, the rolling angle is introduced and proposed, and a modified solution of the torque is proposed. In addition, the model is applied to the prediction of the torque in metro engineering scenarios. The effectiveness of the model is verified and discussed through a comparison of the theoretical solution and field data. Based on the strong correlation between the cutterhead torque and the rolling angle, the calculation method proposed in this paper

is more adaptable to the stratum, more in line with engineering reality, and has higher engineering application value.

2. Project Overview

The total length of the Wuhan Metro Line 8 cross-river tunnel is 3186 m, and the width is about 1500 m, as shown in Figure 1. A slurry TBM with a diameter of 12.51 m is adopted (see Figure 2). The main technical parameters of the shield are shown in Table 1. There are six arms with a spokes panel, and the opening ratio of the cutterhead is about 28.5%. The maximum water and soil pressure is up to 0.7 MPa in this project, and the maximum overburden depth is up to 37 m. The deepest part of the river bottom is 51 m below the normal water level.



Figure 1. Plan of Wuhan Metro Line 8 crosses the Yangtze River.

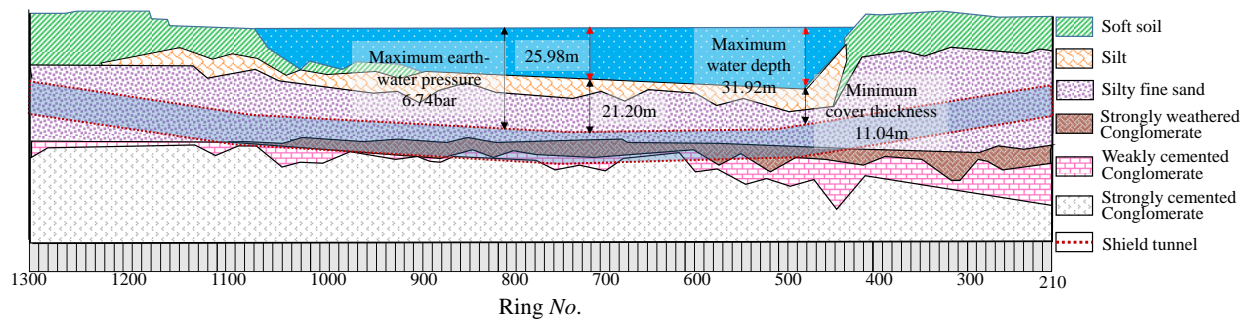


Figure 2. Herrenknecht shield machine (Chutian).

Table 1. Main technical parameters of shield.

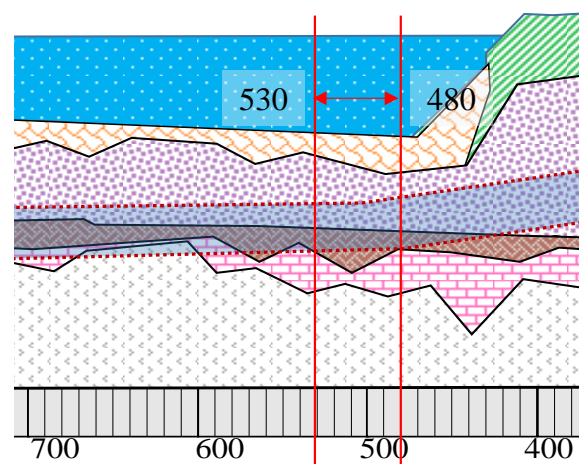
Item	Device Parameter	Engineering Demand
Minimum turning radius	650 m	700 m
Maximum pressure resistance	0.80 Mpa	0.67 Mpa
Maximum gradient	5%	7%
Excavation diameter	12.54 m	14.60
Maximum advancing speed	60 mm/min	60 mm/min
Maximum thrust	156,753 kN	140,000 kN
Maximum torque	18.3~24.6 MN·m	17.2~20.3 MN·m

The slurry TBM needs to traverse the upper soft and lower hard composite stratum for a long distance. The upper part of the tunnel is all silt fine sand. Strongly weathered conglomerate (1365 m) and weakly weathered conglomerate (750 m) are distributed in the middle of the tunnel, and strongly cemented conglomerate is distributed at the bottom of the tunnel, as shown in Figure 3. The project is faced with many technical problems such as soil fracturing and collapse, low excavation efficiency, and attitude deviation [33].

**Figure 3.** Strata profile.

3. Correlation Analysis

Shield rolling angle is an important attitude parameter, but it is often ignored in engineering. Faced with complex strata and high water pressure, there are problems with the cutting of the cutterhead and the difficulty of controlling the torque. Excessive torque results in an excessively large rolling angle. On the other hand, excessive large rolling angle further increases the difficulty of controlling the torque. The rolling angle and torque mutually restrict and influence each other. Therefore, it is necessary to ascertain the inner relationship between the rolling angle and the torque. In this field test, Ring No. 480 to Ring No. 530 was selected as the test tunneling section (see Figure 4).

**Figure 4.** Test tunneling section.

3.1. Measured Data Analysis

According to stratum conditions, in this tunneling section, the designer of the slurry TBM from Herrenknecht set the control line for the positive rolling angle (clockwise) to 5 mm/m, and the control line for the negative rolling angle (counterclockwise) to 10 mm/m based on the Chinese Standard GB 50446-2017 [34]. Through Herrenknecht's own monitoring system, the rolling angle and the cutterhead torque were monitored, and the direction of cutterhead rotation (DCR) during each ring tunneling was recorded (see Figure 5).

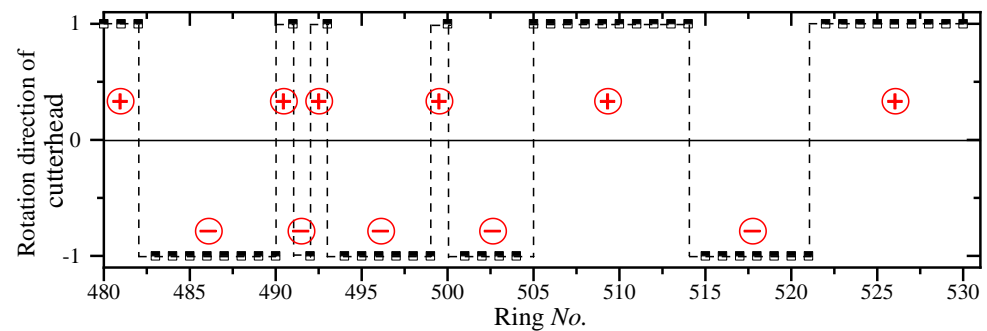


Figure 5. Cutter rotation direction change.

Figure 5 shows the change curve of rolling angle; the rolling angle of the shield is strictly controlled within -10 mm/m to $+5$ mm/m from Ring No. 480 to Ring No. 530. When the rolling angle reaches the control limit value, in the current project, the rolling angle is generally regulated by changing DCR. The change point of DCR is marked in Figure 6. Figure 6 shows that the rolling angle gradually returns to 0 after DCR is changed. It can be observed from Figure 7 that when the DCR has changed, CT will drop rapidly. As shown in Figure 7, the reduction of shield rolling angle can relieve the load-bearing capacity of the shield machine.

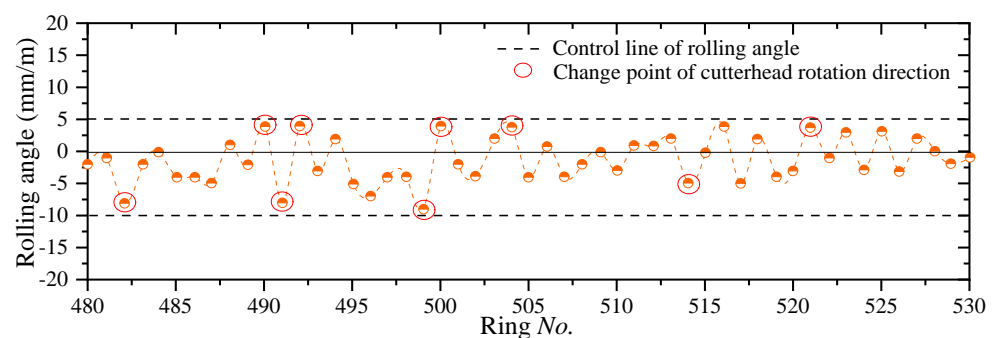


Figure 6. The change curve of the shield rolling angle.

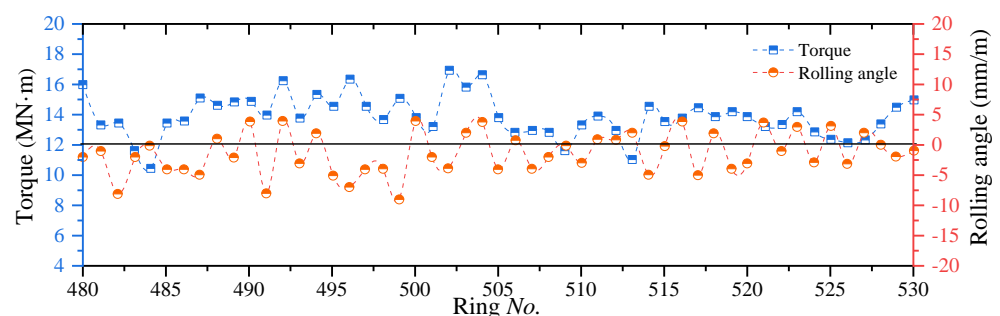


Figure 7. Comparison curve of cutterhead torque and rolling angle.

Through analyzing the changing trend of field data, it can be seen that there is a certain correlation between the rolling angle and CT. Nevertheless, the degree of correlation between the two parameters needs further analysis and discussion.

3.2. Factor Analysis of Torque

CT is affected by soil parameters and shield tunneling parameters. The overall stratum and hydrological conditions of the selected excavation section are similar, so the influence of soil parameters can be ignored, and the impact of tunneling parameters on CT is mainly considered. Xu et al. [35] studied the change law of CT under different thrust, rotation speed and tunneling speed through the excavation model test, but did not consider the influence of the rolling angle on the cutterhead torque. The rotation speed and tunneling speed can be analyzed by the penetration. In this paper, the three variables of penetration, tunneling thrust, and rolling angle are divided into four groups in the form of intervals, as shown in Table 2.

Table 2. Factor level of the cutter torque.

Factor Level	Penetration (mm)	Tunneling Thrust (kN)	Rolling Angle (mm/m)
1	[3.60, 8.00]	[56,691, 61,000]	[0, 1]
2	(8.00, 13.00]	(61,000, 65,000]	(1, 2]
3	(13.00, 18.00]	(65,000, 69,000]	(2, 3.5]
4	(18.00, 23.00]	(69,000, 73,000]	(3.5, 4.5]

The limit value of the positive rolling angle is set as +5 mm/m in the test section, and the negative rolling angle is −10 mm/m. Due to the difference in the absolute value of the positive and negative limit indexes, the following normalization processing has been done:

$$\gamma' = \begin{cases} \gamma\gamma > 0 \\ |\gamma|/2\gamma \leq 0 \end{cases} \quad (1)$$

According to the orthogonal experiment theory, the range is obtained by subtracting the minimum value from the maximum value. It can be observed from Table 3 that the range of the rolling angle is the largest, followed by the penetration, and finally the tunneling thrust, which shows that the CT has the greatest correlation with the rolling angle.

Table 3. Analysis of cutter torque difference (MN·m).

Factor Level	Penetration	Tunneling Thrust	Rolling Angle
1	13.54	13.80	13.44
2	14.56	14.07	13.78
3	14.64	14.26	14.15
4	13.74	13.40	14.60
Extreme differences	1.10	0.86	1.16

According to Table 3, the intuitive analysis results of the relevance of each factor to the torque can be obtained, as shown in Figure 8. It shows the effects of various factors on the torque, and that CT increases with the increasing of the rolling angle. The penetration and tunneling thrust has less influence on the torque. Therefore, it can be judged that the rolling angle has a strong correlation with the CT.

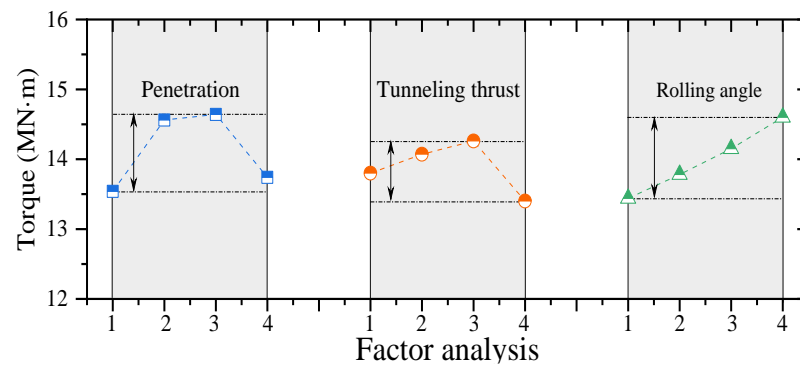


Figure 8. Analysis of factors affecting cutter torque.

3.3. SPSS Analysis

Statistical Product and Service Solutions (SPSS) is a data analysis software. Most of the research on shield tunneling parameters is in the summary stage, and there is no suitable analysis method for the in-depth analysis of tunneling parameters. This paper uses SPSS software to analyze the correlation between the rolling angle, penetration, tunneling thrust, and cutterhead torque [36], and the analysis results are shown in Tables 4–6. When the Sig value is less than 0.01, it indicates that the two variables have a strong correlation, which is represented by two asterisks; if the Sig value is greater than or equal to 0.01 and less than 0.05, it indicates that the two variables have a moderate correlation, which is represented by one asterisk; if the Sig value is greater than or equal to 0.05, it indicates that the two variables are weakly correlated.

Table 4. SPSS Analysis of penetration and cutterhead torque.

Variety	Analysis Results	Penetration	Torque
Penetration	Pearson correlation	1	0.160
	Significant (double tail)		0.261
Torque	Pearson correlation	0.160	1
	Significant (double tail)	0.261	

Table 5. SPSS Analysis of tunneling thrust and cutterhead torque.

Variety	Analysis Results	Tunneling Thrust	Torque
Tunneling thrust	Pearson correlation	1	−0.059
	Significant (double tail)		0.682
Torque	Pearson correlation	−0.059	1
	Significant (double tail)	0.682	

Table 6. SPSS Analysis of rolling angle and cutterhead torque.

Variety	Analysis Results	Rolling Angle	Torque
Rolling angle	Pearson correlation	1	0.391 **
	Significant (double tail)		0.005
Torque	Pearson correlation	0.391 **	1
	Significant (double tail)	0.005	

Note: ** Indicates that at the 0.01 level (two-tailed), the correlation is significant.

According to the analysis results (see Tables 4 and 5), the Sig values between penetration, tunneling thrust, and rolling angle are all greater than 0.05, which shows that the correlation between penetration, thrust and rolling angle is weak. However, it is seen

from Table 6 that the correlation between the rolling angle and CT is significant. Therefore, the theoretical calculation method of CT should consider the influence of rolling angle. Through SPSS analysis, the strong correlation between the rolling angle and the CT is once again proved.

4. Modified Solution of Cutterhead Torque

According to the analysis results in Section 3, the rolling angle has a more significant correlation with CT than other tunneling parameters. In this section, based on the traditional calculation method of the torque, the rolling angle is considered, and a modified solution of the torque is proposed.

4.1. Krause Empirical Model

The Krause empirical load model is widely used in shield design and construction. In 1987, Krause collected and analyzed the construction load data from 397 sets of slurry shield tunneling machines made in Japan and 12 sets made in Germany. He proposed the empirical load model shown in Equation (2) [37,38]:

$$T = \alpha D^3 \quad (2)$$

where T (kN·m) is the total torque; D (m) is the shield diameter; α (kN·m²) is the empirical coefficient that depends on the ground conditions and the type of shield. The range of α , determined by the statistical analysis of in-situ data and widely used in current engineering, is 9 to 23, as shown Figure 9 [19]. The empirical value range of CT in this paper is from 17.75 MN·m to 45.35 MN·m ($D = 12.54$ m).

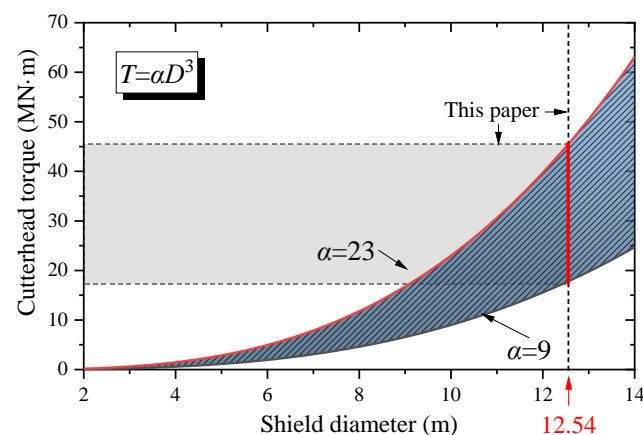


Figure 9. Cutterhead torque of the Krause empirical model.

4.2. Theoretical Calculation Model of Cutterhead Torque

When the shield tunnels in the ground, CT is mainly used to overcome the resistance torque of the formation when the cutterhead cuts the soil (T_1), the friction torque between the front, side, and back of the cutterhead and the soil (T_2), the resistance torque caused by the seal of the cutterhead (T_3), the friction torque caused by the main bearing of the cutterhead (T_4), and the friction loss torque of the reducer (T_5) [18,22]. Therefore, the shield cutterhead torque can be expressed as:

$$T = T_1 + T_2 + T_3 + T_4 + T_5 \quad (3)$$

4.3. Modified Solution Derivation

Table 7 shows the statistics of several shield projects on the torque composition of the cutterhead [39,40]. It shows that CT is mainly composed of overcoming formation resistance and friction. T_1 and T_2 account for about 80–90% of the total torque. Based on

this statistical data, this paper simplified the calculation model due to the unavailability of some shield mechanical parameters, as shown in Equation (4).

$$T = 1.2(T_1 + T_2) \quad (4)$$

Table 7. Related projects.

Project	$T_1 + T_2$ (kN·m)	Total Torque (kN·m)	Percentage (%)
Izmir Metro, Turkey	4297	5289	81.0
London Heathrow Airport Tunnel	13,806	18,842	73.0
Beijing Metro Line 9, China	-	-	91.2
Beijing Metro Line 10, China	-	-	93.8

T_1 and T_2 can be obtained by the following method. During the advancing process of the shield, the resistance torque generated by the cutter cutting the soil is:

$$T_1 = \int_0^{R_0} q_u h_{\max} r dr = 0.5 q_u h_{\max} R_0^2 \quad (5)$$

where q_u is unconfined compressive strength of soil; h_{\max} is maximum cutting depth per revolution of the cutterhead; R_0 is the radius of the outermost tool.

When the cutterhead is cutting, the front and side surfaces of the cutterhead rub against the soil, resulting in frictional resistance torque. The specific calculation formula can be expressed as follows:

$$T_2 = T_{21} + T_{22} \quad (6)$$

$$T_{21} = \int_0^{2\pi} \int_0^{\frac{D_c}{2}} (1 - \xi) f \cdot \sigma_{nf} \cdot r^2 dr d\theta \quad (7)$$

$$T_{22} = \int_0^{2\pi} \frac{D^2}{4} f W p_1 \sin^2 \theta d\theta + \int_0^{2\pi} \frac{D^2}{4} f W K_a p_2 \cos^2 \theta d\theta \quad (8)$$

where T_{21} is the friction torque between the front of the cutterhead and the soil; T_{22} is the friction torque between the side of the cutterhead and the soil. σ_{nf} is the normal earth pressure on the front of the cutterhead; f is the friction coefficient of the soil; ξ is the opening ratio of the cutterhead; r is the turning radius of the cutterhead; θ is the angle between the calculation unit on the cutterhead and the vertical axis (see Figure 10); W is the weight of the shield; p_1 is the vertical pressure acting on the side of the cutterhead, p_2 is the horizontal pressure acting on the side of the cutterhead; K_a is the active earth pressure coefficient.

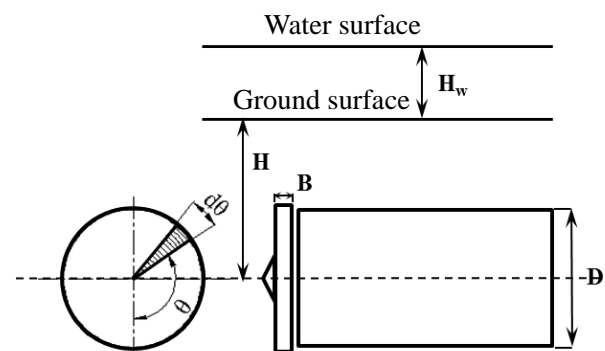


Figure 10. Cutter torque calculation diagram.

The data of rolling angle and cutterhead torque between Ring No. 480 and Ring No. 530 are shown in Figure 10. The points where the rolling angle is greater than 0 and

the points less than or equal to 0 are respectively fitted, and two fitted straight lines are obtained. The fitting parameters are shown in Table 8. As shown in Figure 11, as the rolling angle increases, CT also increases, and the relationship between the two is approximately linear. The theoretical solution of the torque in this area lies between the intercept values of the two straight lines. This is because the theoretical calculation model of CT established does not consider the correlation between rolling angle and torque, and the default is that the rolling angle is 0 mm/m. When the rolling angle reaches +5 mm/m (the set limit value), CT deviation is nearly 20% more than the value obtained from the theoretical model. It has been proved that the rolling angle is a factor that cannot be ignored.

Table 8. Fitting straight parameters.

Fitting Straight Line	Slope	Intercept
Straight line 1 ($\gamma > 0$)	$k_1 = 0.524$	$b_1 = 12.606$
Straight line 2 ($\gamma \leq 0$)	$k_2 = -0.251$	$b_2 = 13.029$

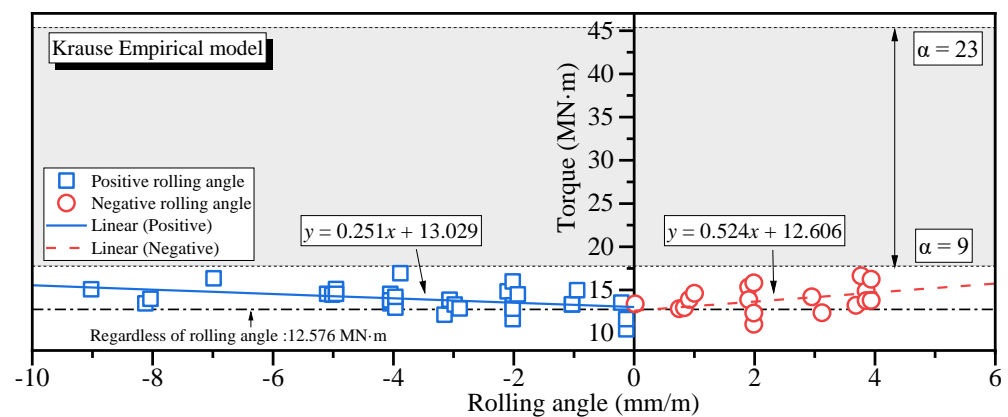


Figure 11. The relationship of shield rolling angle and cutter torque.

Furthermore, it is found that the ratio of k_1 and k_2 has the following relationship with the control line of the rolling angle:

$$\left| \frac{k_1}{k_2} \right| \approx \frac{\gamma^-}{\gamma^+} = 2 \quad (9)$$

where γ^+ is the limit value of the positive rolling angle; and γ^- is the limit value of the negative rolling angle; k_1 and k_2 are the slopes of the fitted straight line respectively.

Therefore, the modified solution of CT is:

$$T^* = \begin{cases} k_1\gamma + T & \gamma > 0 \\ k_2\gamma + T & \gamma \leq 0 \end{cases} \quad k_1\gamma^+ = k_2\gamma^- \quad (10)$$

where T^* is the modified solution of the cutterhead torque.

4.4. Verification

Due to the empirical coefficients β being selected on basis of human experience, a large margin of safety should be required. In comparing the above results with those predicted by the Krause empirical model, the empirical torque range is 141–360% of the average of the field data (see Figure 11). The accuracy of the torque by the proposed model can significantly improves on estimates provided by the empirical model.

The modified solution of CT obtained in Section 4.3 need to be further verified, and the field data of the 10 rings before Ring No. 480 and the 10 rings after the Ring No. 530 are selected for comparison and analysis. Since the selected verification tunneling section is adjacent to the test section, it can be considered that the geological conditions are

similar, and the influence of soil parameters on the torque can almost not be considered. Figure 12 shows the comparison of measured value and theoretical value obtained from this paper method. It can be seen from Figure 12 that the calculated value obtained by the modified solution is more similar to the measured value, and there is a small gap between the calculated and measured value.

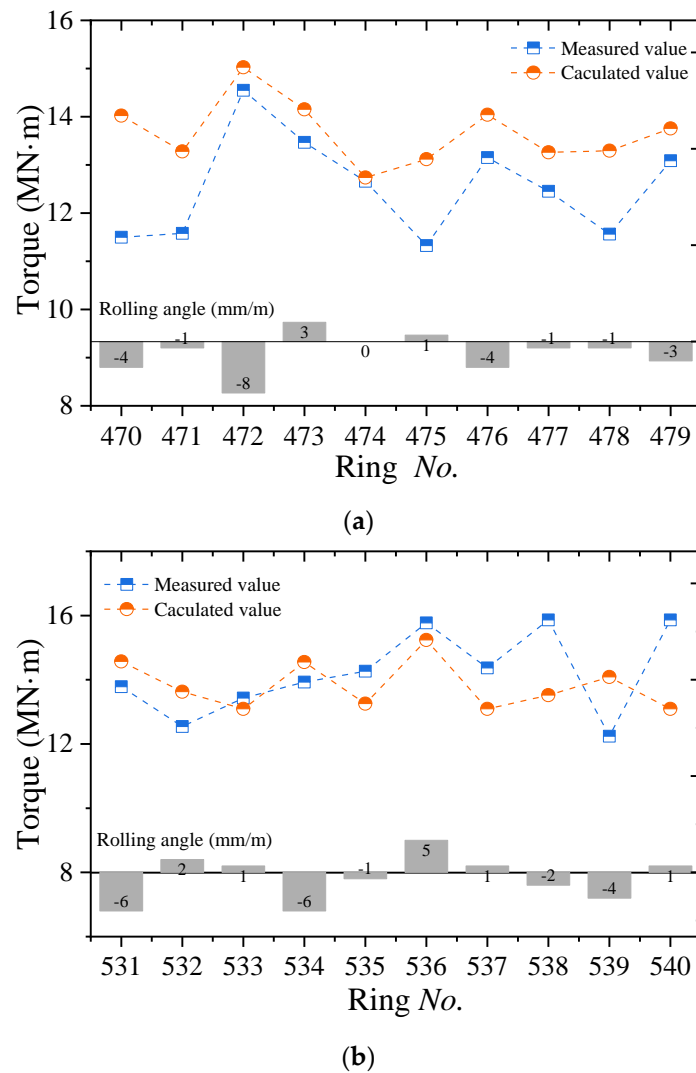


Figure 12. Comparison of measured value and theoretical value: (a) Ring No.470~ Ring No.479; (b) Ring No.531~ Ring No.540.

CT can generally reflect the difficulty of tunneling and the operating status of the shield. Therefore, accurately predicting the torque of the cutterhead can ensure the continuous and safe construction of the shield machine. The modified solution proposed in this paper can avoid complicated mechanical calculations with changes in ground conditions, and is more suitable for the prediction and control of cutterhead torque in actual engineering construction. Figure 13 presents the mean absolute percentage error (MAPE) values of the two verification intervals [41]. The MAPE expression can be obtained by Equation (11). The MAPE values are 8.476% and 8.268%, respectively, and those MAPE values can basically meet the actual application requirements of the project.

$$\text{MAPE} = \frac{1}{n} \sum_{i=1}^n \left| \frac{r_i - p_i}{r_i} \right| \times 100\% \quad (11)$$

where r is the measured value; p is the calculated value; n is total number of datasets.

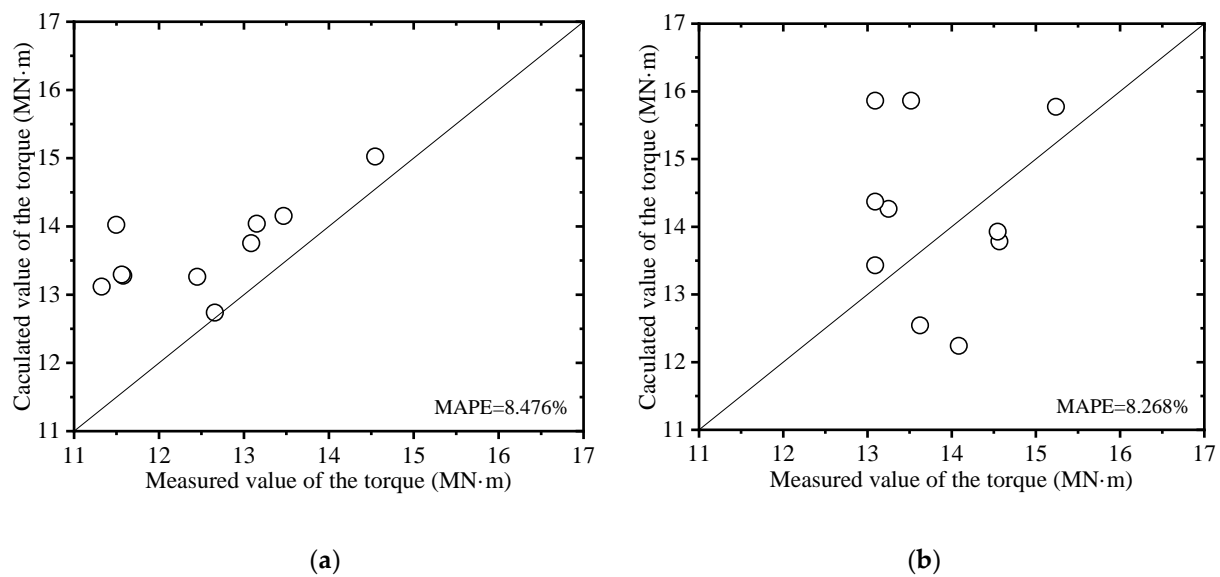


Figure 13. Error Analysis: (a) Ring No.470~ Ring No.479; (b) Ring No.531~ Ring No.540.

Figure 14 shows the relationship between the rolling angle and CT (Ring No. 630–650). The rolling angle and the torque in this tunneling section are similar to those of the tunneling section between Ring No. 480 and Ring No. 530. The slope of the fitted straight line can also be used to draw up the control line for the rolling angle in the adjacent tunneling section. The k_1 value of this tunneling section is similar to the k_1 value of the tunneling section (Ring No. 480–530), so γ^+ is still taken as +5 mm/m. According to the ratio of k_1 and k_2 , γ^- should be set as −8 mm/m. This indicates that the control range of the rolling angle should be reduced, and CT is regulated more strictly in this area.

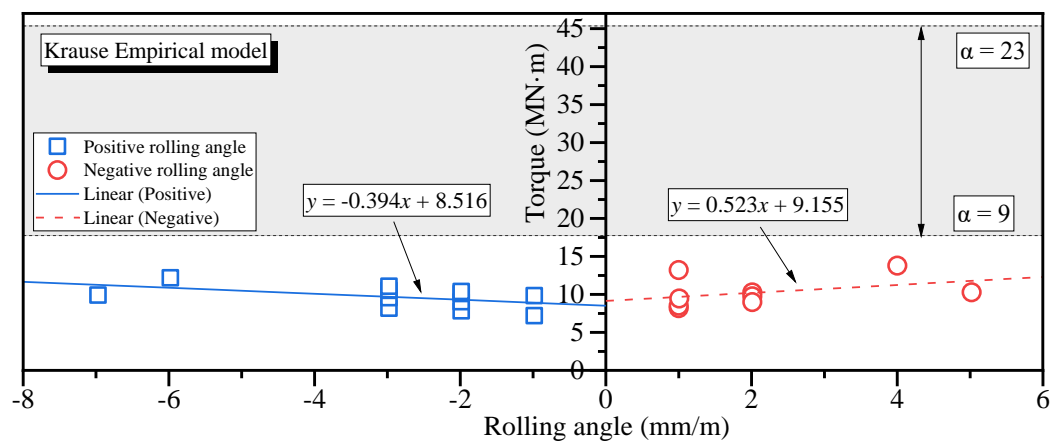


Figure 14. The relationship of shield rolling angle and cutter torque diagram (Ring No. 630–Ring No. 650).

It can be seen from the geological section (see Figure 3) that there are upper soft and lower hard strata in this section, and the proportion of the hard rock occupying the extraction face is higher than that of the tunneling section from Ring No. 630 to Ring No. 650. The geological conditions of this tunneling section are more complicated, and the shield tunneling parameters are more difficult to control. The shield tunneling is relatively difficult, and CT is more difficult to control. Therefore, it is necessary to reduce the control range of the shield rolling angle.

5. Conclusions

Through the range and SPSS analysis methods, it is proved in this paper that the cutterhead torque has a strong correlation with the rolling angle. On the basis of the theoretical solution of the torque, a modified solution considering the rolling angle is obtained. The main conclusions from this study are enumerated below.

(1) Ring No. 480 to Ring No. 530 are selected as the test tunneling section, and the field data are analyzed. The results shows that the rolling angle is strictly controlled within a limited range, and can be reduced gradually to 0 mm/m by changing DCR.

(2) The three variables of penetration, thrust, and rolling angle are selected for interval grouping. Through range and SPSS analysis methods, it is proved that the rolling angle has a stronger correlation with CT than the other two factors.

(3) Based on the theoretical calculation model of CT, and through regression analysis of the field data, the modified solution of CT considering the rolling angle is obtained. Using this calculation method, the prediction accuracy of CT is much higher than that of the traditional K model. Compared with the existing theoretical calculation methods, the predicted value obtained by the method proposed in this paper is more in line with the actual engineering.

Due to the limited collection of engineering cases, the cutterhead torque calculation method proposed in this paper only verifies the tunneling parameters of this project, and some useful conclusions have been obtained. However, in the future, it is necessary to collect more comprehensive engineering data to further verify the rationality of this method.

6. Patents

This section is not mandatory but may be added if there are patents resulting from the work reported in this manuscript.

Author Contributions: Investigation and methodology, X.S. and C.C.; conceptualization, D.Y.; validation, D.J. All authors have read and agreed to the published version of the manuscript.

Funding: This research was funded by the National Natural Science Foundation of China (Grant Nos. 52090084, 52108377, 51938008) and China Postdoctoral Science Foundation (2021M702269, 2021T140474).

Institutional Review Board Statement: Not applicable.

Informed Consent Statement: Not applicable.

Data Availability Statement: Not applicable.

Conflicts of Interest: The authors declare that they have no known competing financial interests or personal relationships that could have appeared to influence the work reported in this paper.

References

1. Qian, Q.H.; Lin, P. Safety risk management of underground engineering in China: Progress, challenges and strategies. *J. Rock Mech. Geotech.* **2016**, *8*, 423–442. [\[CrossRef\]](#)
2. Chen, X.S. Research on combined construction technology for cross-metro tunnels in underground spaces. *Engineering* **2018**, *4*, 103–111. [\[CrossRef\]](#)
3. Shen, X.; Yuan, D.J.; Cao, L.Q.; Jin, D.; Chen, X.; Gao, Z. Experimental investigation of the failure of shield grease seals under the influence of environmental factors: A case study. *Eng. Fail. Anal.* **2022**, *133*, 105975. [\[CrossRef\]](#)
4. Jin, D.L.; Zhang, Z.Y.; Yuan, D.J. Effect of dynamic cutterhead on face stability in EPB shield tunneling. *Tunn. Undergr. Space Technol.* **2021**, *110*, 103827. [\[CrossRef\]](#)
5. Shen, X.; Yuan, D.J.; Jin, D.L. Influence of shield attitude change on shield–soil interaction. *Appl. Sci. Basel* **2019**, *9*, 1812. [\[CrossRef\]](#)
6. Liu, J.; Li, P.N.; Shi, L.; Fan, J.; Kou, X.Y.; Huang, D.Z. Spatial distribution model of the filling and diffusion pressure of synchronous grouting in a quasi-rectangular shield and its experimental verification. *Undergr. Space* **2021**, *6*, 650–664. [\[CrossRef\]](#)
7. Jin, Y.R.; Qin, C.J.; Tao, J.F.; Liu, C.L. An accurate and adaptative cutterhead torque prediction method for shield tunneling machines via adaptative residual long-short term memory network. *Mech. Syst. Sig. Process.* **2022**, *165*, 108312. [\[CrossRef\]](#)
8. Li, S.H.; Zhang, M.J.; Li, P.F. Analytical solutions to ground settlement induced by ground loss and construction loadings during curved shield tunneling. *J. Zhejiang Univ. Sci. A* **2021**, *22*, 296–313. [\[CrossRef\]](#)

9. Han, M.D.; Cai, Z.X.; Qu, C.Y. Dynamic numerical simulation of cutterhead loads in TBM tunnelling. *Tunn. Undergr. Space Technol.* **2017**, *70*, 286–298. [\[CrossRef\]](#)
10. Jin, D.L.; Yuan, D.J.; Li, X.G.; Su, W. Probabilistic analysis of the disc cutter failure during TBM tunneling in hard rock. *Tunn. Undergr. Space Technol.* **2021**, *109*, 103744. [\[CrossRef\]](#)
11. Tao, Y.; Shen, S.L.; Zhou, A.N.; Lyu, H.-M. Construction efficiency of shield tunnelling through soft deposit in Tianjin, China. *Tunn. Undergr. Space Technol.* **2021**, *112*, 103917.
12. Askildrud, O.; Moulton, B. *Tunnel Boring Machines. Mechanical Tunnelling. Raise Boring and Shaft Drilling Short Course*; Colorado School of Mines: Golden, CO, USA, 1998.
13. Maidl, B.; Herrenknecht, M.; Maidl, U.; Wehrmeyer, G.; Sturge, D.S. *Mechanised Shield Tunneling*, 2nd ed.; John Wiley & Sons: Hoboken, NJ, USA, 2013.
14. Reilly, B.J. EPBs for the north east line project. *Tunn. Undergr. Space Technol.* **1999**, *14*, 491–508. [\[CrossRef\]](#)
15. Zhang, Q.; Hou, Z.D.; Huang, G.Y.; Cai, Z.X.; Kang, Y. Mechanical characterization of the load distribution on the cutterhead–ground interface of shield tunneling machines. *Tunn. Undergr. Space Technol.* **2015**, *47*, 106–113. [\[CrossRef\]](#)
16. Faramarzi, L.; Kheradmandian, A.; Azhari, A. Evaluation and Optimization of the Effective Parameters on the Shield TBM Performance: Torque and Thrust—Using Discrete Element Method (DEM). *Geotech. Geol. Eng.* **2020**, *38*, 2745–2759. [\[CrossRef\]](#)
17. Shi, H.; Yang, H.Y.; Gong, G.F. Determination of the cutterhead torque for EPB shield tunneling machine. *Autom. Constr.* **2011**, *20*, 1087–1095. [\[CrossRef\]](#)
18. Wang, L.T.; Gong, G.F.; Shi, H.; Yang, H. Modeling and analysis of thrust force for EPB shield tunneling machine. *Automat. Constr.* **2012**, *27*, 138–146. [\[CrossRef\]](#)
19. Zhang, Q.; Qu, C.Y.; Cai, Z.X. Modeling of the thrust and torque acting on shield machines during tunneling. *Automat. Constr.* **2014**, *40*, 60–67. [\[CrossRef\]](#)
20. Ates, U.; Bilgin, N.; Copur, H. Estimating torque, thrust and other design parameters of different type TBMs with some criticism to TBMs used in Turkish tunneling projects. *Tunn. Undergr. Space Technol.* **2014**, *40*, 46–63. [\[CrossRef\]](#)
21. González, C.; Arroyo, M.; Gens, A. Thrust and torque components on mixed-face EPB drives. *Tunn. Undergr. Space Technol.* **2016**, *57*, 47–54. [\[CrossRef\]](#)
22. Zhou, X.P.; Zhai, S.F. Estimation of the cutterhead torque for earth pressure balance TBM under mixed-face conditions. *Tunn. Undergr. Space Technol.* **2018**, *74*, 217–229. [\[CrossRef\]](#)
23. Zhang, K.; Lyu, H.M.; Shen, S.L.; Zhou, A. Evolutionary hybrid neural network approach to predict shield tunneling-induced ground settlements. *Tunn. Undergr. Space Technol.* **2020**, *106*, 103594. [\[CrossRef\]](#)
24. Khotbehsara, M.M.; Manalo, A.; Aravinthan, T.; Ferdous, W. Synergistic effects of hygrothermal conditions and solar ultraviolet radiation on the properties of structural particulate-filled epoxy polymer coatings. *Constr. Build. Mater.* **2021**, *277*, 122336. [\[CrossRef\]](#)
25. Yu, P.; Manalo, A.; Ferdous, W.; Abousnina, R.; Salih, C.; Heyer, T.; Schubel, P. Investigation on the physical, mechanical and microstructural properties of epoxy polymer matrix with crumb rubber and short fibres for composite railway sleepers. *Constr. Build. Mater.* **2021**, *295*, 123700. [\[CrossRef\]](#)
26. Zhao, R.; Yan, R.Q.; Chen, Z.H.; Mao, K.; Wang, P.; Gao, R.X. Deep learning and its applications to machine health monitoring. *Mech. Syst. Sig. Process.* **2019**, *115*, 213–237. [\[CrossRef\]](#)
27. Armaghani, D.J.; Koopialipoor, M.; Marto, A.; Yagiz, S. Application of several optimization techniques for estimating TBM advance rate in granitic rocks. *J. Rock Mech. Geotech. Eng.* **2019**, *11*, 779–789. [\[CrossRef\]](#)
28. Sun, W.; Shi, M.L.; Zhang, C.; Zhao, J.; Song, X. Dynamic load prediction of tunnel boring machine (TBM) based on heterogeneous in-situ data. *Autom. Constr.* **2018**, *92*, 23–34. [\[CrossRef\]](#)
29. Gao, X.J.; Shi, M.L.; Song, X.G.; Zhang, C.; Zhang, H. Recurrent neural networks for real-time prediction of TBM operating parameters. *Autom. Constr.* **2019**, *98*, 225–235. [\[CrossRef\]](#)
30. Luo, W.P.; Yuan, D.J.; Jin, D.L.; Lu, P.; Chen, J. Optimal Control of Slurry Pressure during Shield Tunnelling Based on Random Forest and Particle Swarm Optimization. *CMES-Comp. Model. Eng.* **2021**, *128*, 109–127. [\[CrossRef\]](#)
31. Qin, C.J.; Shi, G.; Tao, J.F.; Honggan, Y.; Yanrui, J.; Junbo, L.; Chengliang, L. Precise cutterhead torque prediction for shield tunneling machines using a novel hybrid deep neural network. *Mech. Syst. Signal. Process.* **2021**, *151*, 107386. [\[CrossRef\]](#)
32. Shi, G.; Qin, C.J.; Tao, J.F.; Liu, C. A VMD-EWT-LSTM-based multi-step prediction approach for shield tunneling machine cutterhead torque. *Knowl. Based Syst.* **2021**, *228*, 107213. [\[CrossRef\]](#)
33. Wang, T.; Yuan, D.J.; Jin, D.L.; Li, X. Experimental study on slurry-induced fracturing during shield tunneling. *Front. Struct. Civ. Eng.* **2021**, *15*, 333–345. [\[CrossRef\]](#)
34. GB 50446—2017. *Code for Construction and Acceptance of Shield Tunneling Method*; Ministry of Housing and Urban-Rural Construction of the People's Republic of China: Beijing, China, 2017.
35. Xu, Q.W.; Zhu, H.H.; Ding, W.Q.; Ge, X. Laboratory model tests and field investigations of EPB shield machine tunneling in soft ground in Shanghai. *Tunn. Undergr. Space Technol.* **2011**, *26*, 1–14. [\[CrossRef\]](#)
36. Sabzi, S.; Javadikia, P.; Rabani, H.; Adelkhani, A. Mass modeling of Bam orange with ANFIS and SPSS methods for using in machine vision. *Measurement* **2013**, *46*, 3333–3341. [\[CrossRef\]](#)
37. Krause, T. Schildvortrieb mit Flüssigkeits und Erdgestützter Ortsbrust. In *Mitteilung des Instituts für Grundbau und Bodenmechanik*; TU Braunschweig: Braunschweig, Germany, 1987; p. 624. (In German)

-
38. Maidl, B.; Herrenknecht, M.; Anheuser, L. *Mechanised Shield Tunneling*; Ernst & Sohn: Berlin, Germany, 1996.
 39. Jiang, H.; Jiang, Y.S.; Zhang, J.X.; Cheng, X.W.; Yang, Z.Y. Research on cutterhead torque during earth pressure balance shield tunneling in sand gravel of Beijing metro. *China Railw. Sci.* **2013**, *34*, 59–65. (in Chinese).
 40. Li, C.; Zhou, H.W.; Zuo, J.P.; Ding, J.; Gao, M.; Shuai, Q. Torque calculation method of cutterhead in earth pressure balance shield and quantitative analysis of several influencing factors. *Chin. J. Rock Mech. Eng.* **2013**, *32*, 760–766. (In Chinese)
 41. Hyndman, R.J.; Koehler, A.B. Another look at measures of forecast accuracy. *Int. J. Forecast.* **2006**, *22*, 679–688. [[CrossRef](#)]